A Procedure for Identifying Planes and Axes of Symmetry Candidates in B-rep CAD Models

Mladen Buric[1] [ID] and Stanko Skec[2] [ID]

[1]University of Zagreb, mladen.buric@fsb.hr
[2]University of Zagreb, stanko.skec@fsb.hr

Corresponding author: Mladen Buric, mladen.buric@fsb.hr

Abstract. Computer-Aided Symmetry Detection (CASD) supports mechanical engineers in detecting the planes and axes of symmetry in 3D CAD models. A common approach of many CASD techniques is first to create a set of planes of symmetry candidates (POSCs) and axes of symmetry candidates (AOSCs), which are then evaluated to identify the actual planes and axes of symmetry among them. The candidates are often identified from the input model's geometry by pairing entities (e.g., point clouds, surfaces, mesh triangles, etc.). Consequently, a considerable number of candidates may be generated without their practical need to detect symmetries, thus making the CASD computationally demanding. Hence, this study proposes a procedure for identifying a reduced number of POSCs and AOSCs to detect exact global and partial axis- and reflectional symmetry in 3D CAD models with Boundary Representation.

1   INTRODUCTION

Symmetry is a geometrical property beneficial in many applications in mechanical engineering [11][15][20][26][28]. In mechanical design, during solid modeling, 3D CAD models are often shaped symmetrically for different reasons: to simplify the modeling process, to reduce the complexity of assemblies and the number of unique parts [6], or to minimize assembly errors and assembly time [26]. Symmetry information (i.e., the planes and axes of symmetry) is often not explicitly stored in native 3D CAD models unless the final shape of the model is created using mirroring or pattern operations. The *neutral* exchange file formats currently also do not support storing any symmetry information. Therefore, the existence of symmetry in the 3D CAD models is usually checked and recognized visually by mechanical engineers. However, this may be a tedious and time-consuming task, especially if the 3D CAD model's shape is geometrically complex or consists of a large number of topological entities. Thus, *Computer-Aided Symmetry Detection*

(CASD) is preferred, which supports mechanical engineers in detecting the symmetry information in the 3D CAD models.

A common approach of many CASD techniques [1][2][5][7]-[9][11]-[13][16][22]-[27] is to identify a set of *planes of symmetry candidates* (POSCs) and/or *axes of symmetry candidates* (AOSCs) and to evaluate the existence of the *actual planes of symmetry* (APOS) and/or *actual axes of symmetry* (AAOS) among them. The candidates are usually identified by Principal Component Analysis [1][2][13][24][25], through the pairing of entities (e.g., points, mesh triangles, loops, viewpoints, etc.) [5][8][23][26][27], from the shape's generalized moment functions [16], intrinsic surface properties [11][12], by incremental rotations around the centroid [31], etc. The POSCs and/or AOSCs are evaluated by applying corresponding transformations (reflection, rotation, etc.) on the input model with respect to each candidate [8][22][25], steepest descent minimization [16], voting algorithms [9][23], Hausdorff distance and ray casting [24], matching viewpoint entropy values [13], candidate sorting and ranking [26][27], candidate propagation process over topological entities [11][12], a vector-based calculation procedure [1][2], etc. Alternatively, the APOSs or AAOSs can be detected directly without the generation of candidates. For instance, by clustering points obtained through searching candidate point transformations [18], applying spectral analysis to the symmetry correspondence matrix (which encodes symmetry relations between pairs of n points sampled from the input data) [14], applying optimization to spherical harmonic coefficients that approximate the shape [10], etc.

This study is exclusively focused on the stage of CASD that deals with the identification of POSCs and AOSCs in 3D CAD models with Boundary Representation (B-rep). Identifying too many POSCs and AOSCs without their practical need for detecting symmetries can result in a computationally demanding CASD evaluation procedure [6]. On the other hand, identifying too few POSCs and AOSCs increases the risk of symmetry detection failure. Hence, this study proposes a procedure for identifying a reduced number of POSCs and AOSCs to detect exact global and partial axi- and reflectional symmetry.

2 RELATED WORK

2.1 Identification of POSCs and AOSCs in B-rep CAD Models

The existing studies obtained the POSCs and AOSCs from the B-rep's topological elements (e.g., loops, faces, etc.) and their underlying geometrical properties [11][12][26][27] and principal axes of inertia [1][2]. *Li et al.* [11][12] identified the POSCs and AOSCs from one, two, or three adjacent faces using the intrinsic parameters of the underlying surfaces and their intersections (vertices, edges, and loops). For instance, the intrinsic parameters of a plane surface are its base point and normal vector, those of a cylindrical surface its axis point, axis vector and radius, and so on. The AOSCs were considered a special case of an infinite number of POSCs. For example, axisymmetric faces (e.g., a closed cylinder, sphere, etc.) have an infinite number of POSCs. Then, a two-level propagation process of the candidates over the B-rep model was used to determine the global or local symmetries of exact and partial axi- and reflectional symmetric 3D CAD models. The highest possible number of candidates n_C (including POSCs and AOSCs) corresponds to the following equation [12]:

$$n_C = 2n_E + pn_V + n_L ,$$ (1.1)

where n_E represents the total number of edges, n_V is the total number of vertices, and n_L is the total number of loops in the 3D CAD model, while parameter p parameter describes the maximum number of adjacent faces around a vertex (therefore, $p=4$ can be assumed). The drawback of the study is that a combinatorial analysis was used to obtain the combinations of surfaces, their adjacencies, and intersections for identifying the POSCs and AOSCs. In addition, the study addresses only analytic surfaces (plane, cylinder, cone, sphere, and torus). Consequently, if the 3D CAD model contains some non-predicted combinations of analytic surfaces or any numeric surfaces (e.g., B-spline), the corresponding POSCs or AOSCs may remain undetected. The study by *Buric et*

al. [1][2] proposed using three POSCs and three AOSCs aligned with the principal axes of inertia and passing through the center of gravity (COG). The CASD did not apply to partial symmetric 3D CAD models or those exhibiting exact reflectional symmetries misaligned with the principal axes of inertia. The study by *Tate et al.* [26][27] identified the POSCs by pairing identical loops of the same type through their geometric properties (e.g., loop area, number of edges, etc.), while the AOSCs were identified from single loops. The loop type is dependent on the surface type (plane, cylinder, sphere, torus, cone, etc.). Then, duplicate POSCs and AOSCs were rationalized, i.e., eliminated by comparison of their location and orientation. The maximum number of POSCs and AOSCs equals [27]:

$$n_C = n_{POSC} + n_{AOSC} = \sum \frac{n_{L,i}(n_{L,i} - 1)}{2} + n_E , \qquad (1.2)$$

where $n_{L,i}$ represents the total number of loops of the particular loop type, and the sum indicates that they are all added together. The POSCs and AOSCs have been used to detect global exact and partial axi- and reflectional symmetry. In addition, the primary axes (major and minor), which lie parallel and perpendicular to the longest dimension of the 3D CAD model's smallest bounding box, were detected from the intersection of two POSCs with the largest share of loop areas. The obstacle of this study is that the proposed similarity criterion is not adequate as two non-identical topological elements (in this case loops) can have the same geometrical properties (e.g., loop area, number of edges, etc.). Instead of that, the present paper investigates the use of similarity measures for identifying similar topological elements in the B-rep CAD models.

2.2 Similarity Measures

In general, similarity has been studied in mechanical design to support designers in generating new designs [4], or in manufacturing to extract existing product information such as cost estimations in machining [3]. Moreover, recognizing similarities in 3D CAD models may be beneficial for the reuse of existing design solutions [30]. Thereby, a given input CAD model (new design) is used to retrieve similar CAD models from the database (existing designs). Further, recognizing similarity may be exploited for the clustering of CAD models [29]. This study is, however, focused on how to identify similar topological elements (faces) from the B-rep. For that purpose, common similarity measures from statistics are investigated, which are generally used to compare the similarity between two finite data sets. For instance, the *Cosine similarity* (CS) computes the cosine of the angle between two feature vectors A and B:

$$CS = \cos \theta = \frac{\mathbf{A} \cdot \mathbf{B}}{\|\mathbf{A}\| \|\mathbf{B}\|} = \frac{|X \cap Y|}{\sqrt{|X| \cdot |Y|}} = \frac{c}{\sqrt{a + c} \cdot b + c} . \qquad (1.3)$$

The CS can also be expressed in terms of two datasets X and Y. In that case, it is defined as the size of the *intersection* (the number of common elements) divided by the square root of the multiplied cardinalities of the sets. The cardinality of a set, $|X|$ or $|Y|$, represents the number of elements it contains. Alternatively, if two finite data sets are represented by two binary feature vectors A and B, then in the above equation a represents the total number of features with the value 1 in A and 0 in B, b the total number of features with the value 0 in A and 1 in B, and c the total number of features with value 1 in both A and B. For instance, CS was utilized to compute the similarity between two Opitz code vectors (the CAD model features were presented by alphanumerical digits) [30]. Another common similarity measure, the *Jaccard index* (JI), is defined as the size of the *intersection* divided by the size of the *union* (the number of unique elements) of two finite data sets X and Y:

$$JI = \frac{|X \cap Y|}{|X \cup Y|} = \frac{|X \cap Y|}{|X| + |Y| - |X \cap Y|} = \frac{c}{a + b + c} . \qquad (1.4)$$

The JI was employed for clustering purposes to measure the similarity between machines/parts and group them together [21]. Alternative similarity measures related to the Jaccard index are the *Sørensen–Dice coefficient* (SDC), which is defined as twice the size of the intersection divided by

the sum of elements in each set, the *Szymkiewicz–Simpson coefficient* (SSC) or *Overlap coefficient*, described as the ratio between the size of the intersection and the smaller cardinality of two data sets, and the *Braun-Blanquet coefficient* (BBC), which represents the size of the intersection divided by the larger cardinality of two data sets:

$$\text{SDC} = \frac{2 \cdot |X \cap Y|}{|X| + |Y|} = \frac{|X \cap Y|}{0.5 \ |X| + |Y|} = \frac{c}{0.5 \ a + b + 2c} \ , \tag{1.5}$$

$$\text{SSC} = \frac{|X \cap Y|}{\min \ |X|, |Y|} = \frac{c}{\min \ a + c, b + c} \ , \tag{1.6}$$

$$\text{BBC} = \frac{|X \cap Y|}{\max \ |X|, |Y|} = \frac{c}{\max \ a + c, b + c} \ . \tag{1.7}$$

The mentioned similarity measures from Equations (1.3) to (1.7) range between 0 (non-similar) and 1 (absolutely similar). The referred similarity measures are explored in terms of their possibilities and applicability for detecting similar pairs of topological elements which are then used to obtain the POSCs.

3   A PROCEDURE FOR IDENTIFYING PLANES AND AXES OF SYMMETRY CANDIDATES

The proposed procedure for identifying the POSCs and AOSCs addresses the mentioned drawbacks of the CASD technique in [1]. It utilizes a combination of three approaches to obtain the candidates: from *single faces*, *similar face pairs,* and the *principal axes of inertia*. Generally, the identified POSCs are intended for detecting reflectional symmetry, while the identified AOSCs are intended for detecting axisymmetry. The proposed procedure consists of two main phases: *generating* and *trimming* the POSCs and AOSCs. The initial set of POSCs is *generated* through the pairing of similar faces, but only of the plane surface type, while the initial set of AOSCs is generated from single faces with the underlying cylindrical surface type. In addition, three POSCs and three AOSCs are always generated from the principal axes of inertia to cover possible exact symmetries that are aligned with the principal axes. The procedure for computing the principal axes of inertia is given in the paper [1].

Face pairs are generated by joining all faces of the plane surface type with each other. Then, all face pairs are looped and each of them is subjected to a quick filtering step where the ratio between the surface areas needs to be $A_i / A_j \geq A_{TH}$ ($A_i \leq A_j$) to proceed to the computation of the similarity measure. The A_{TH} represents the threshold value which shall be determined later in this paper from test cases. The quick filtering step is important for the elimination of face pairs that have a considerable difference in terms of surface area and are, therefore, not likely to be similar. Consequently, the computational effort of the analysis can be reduced. Then, for each filtered face pair, the similarity measure is computed and compared with the threshold value S_{TH}. If the similarity measure score is 1, the face pair is considered similar, and the location of the POSC is determined from the midpoint M between the two face centroids:

$$M(x_M, y_M, z_M) = \left(\frac{x_{C_1} + x_{C_2}}{2}, \frac{y_{C_1} + y_{C_2}}{2}, \frac{z_{C_1} + z_{C_2}}{2} \right), \tag{1.8}$$

If the similarity measure score is $> S_{TH}$ and < 1, then the midpoint between the faces is computed from the face centers C_1' and C_2', which represent the average position of the midpoints of edges that are identical and shared by a face pair:

$$M(x_M, y_M, z_M) = \left(\frac{x_{C_1'} + x_{C_2'}}{2}, \frac{y_{C_1'} + y_{C_2'}}{2}, \frac{z_{C_1'} + z_{C_2'}}{2} \right), \tag{1.9}$$

where

$$C_1{}'(x_{C_1{}'}, y_{C_1{}'}, z_{C_1{}'}) = \left(\frac{1}{n_{E_1}} \sum_{i=1}^{n_{E_1}} x_{E_{1\,i,m}}, \frac{1}{n_{E_1}} \sum_{i=1}^{n_{E_1}} y_{E_{1\,i,m}}, \frac{1}{n_{E_1}} \sum_{i=1}^{n_{E_1}} z_{E_{1\,i,m}} \right), \tag{1.10}$$

$$C_2{}'(x_{C_2{}'}, y_{C_2{}'}, z_{C_2{}'}) = \left(\frac{1}{n_{E_2}} \sum_{j=1}^{n_{E_2}} x_{E_{2\,j,m}}, \frac{1}{n_{E_2}} \sum_{j=1}^{n_{E_2}} y_{E_{2\,j,m}}, \frac{1}{n_{E_2}} \sum_{j=1}^{n_{E_2}} z_{E_{2\,j,m}} \right), \tag{1.11}$$

where $n_{E_1} = n_{E_2}$ represent the number of identical edges shared by a face pair, $x_{E_{1\,i,m}}$, $y_{E_{1\,i,m}}$, & $y_{E_{1\,i,m}}$ are the midpoint coordinates of the *i*-th edge in first face, while $x_{E_{2\,j,m}}$, $y_{E_{2\,j,m}}$, & $y_{E_{2\,j,m}}$ are the midpoint coordinates of the *j*-th edge in second face. The orientation of the POSC depends on the arrangement between the two faces, which may be *parallel*, *coplanar*, or *arbitrarily angled*. If two faces are parallel, the POSC's orientation is equal to the normal vector of either one of the faces:

$$\vec{n}_{\text{POSC}}(a,b,c) = \vec{n}_1 \text{ or } \vec{n}_{\text{POSC}}(a,b,c) = \vec{n}_2 . \tag{1.12}$$

If two faces are coplanar, the orientation of the POSC corresponds to the vector between the face centroid C_1 and face centroid C_2:

$$\vec{n}_{\text{POSC}}(a,b,c) = \left(\frac{x_{C_1} - x_{C_2}}{2}, \frac{y_{C_1} - y_{C_2}}{2}, \frac{y_{C_1} - y_{C_2}}{2} \right). \tag{1.13}$$

Finally, if two faces are arbitrarily angled, the POSC's orientation is obtained by subtracting the normal vectors of the two faces:

$$\vec{n}_{\text{POSC}}(a,b,c) = \vec{n}_1 - \vec{n}_2 . \tag{1.14}$$

Axisymmetric parts (exact or partial) are predominantly made of cylindrical surfaces that contribute to symmetry. Hence, the initial set of AOSCs can be generated by simply looping all faces of the cylindrical surface type in the 3D CAD model. Each AOSC is defined by its origin point and cylinder's axis direction vector and can be retrieved from the cylinder properties. The initially generated POSCs and AOSCs need to be further processed in the *trimming* phase where first duplicates, i.e., coincident candidates, are removed. Then, the point-to-plane distance (PTPD) is computed for each POSC, and the point-to-line distance (PTLD) for each AOSC, to assess their distances from the COG. It is known that if an object has exact global symmetries, its planes and/or axes of symmetry will pass through the COG [17][26]. In the case of partial symmetrical objects, the POS and/or AOS will be close to the COG [19]. The PTPD d_{PTPD} and PTLD d_{PTLD} are calculated using the following equations:

$$d_{\text{PTPD}} = \frac{\left| ax_{\text{COG}} + by_{\text{COG}} + cz_{\text{COG}} - (ax_M + by_M + cz_M) \right|}{\sqrt{a^2 + b^2 + c^2}} \le d_{\max} , \tag{1.15}$$

$$d_{\text{PTLD}} = \frac{\left\| \vec{PC} \times \vec{a} \right\|}{\left\| \vec{a} \right\|} \le d_{\max} , \tag{1.16}$$

where P is any point on the axis (e.g., the origin point), point $C(x_{\text{COG}}, y_{\text{COG}}, z_{\text{COG}})$ is the COG, and $\vec{a}$ the cylinder's axis direction vector. Both distances need to be below $d_{\max}$, which is the maximum allowable distance of the candidate from the COG. Any candidate that is too far distanced from the COG is being removed from further analysis. Finally, the trimmed POSC and AOSC are used as input for the *symmetry detection* procedure to identify the APOS or AAOS, which is beyond the scope of this study. The largest possible number of POSCs and AOSCs in the 3D CAD model before trimming equals:

$$n_{\text{POSC}} = \frac{n_{\text{PL}} (n_{\text{PL}} - 1)}{2} + 3 , \tag{1.17}$$

$$n_{\text{AOSC}} = n_{\text{CY}} + 3 , \tag{1.18}$$

where n_{PL} is the total number of faces of the plane surface type and n_{CY} is the total number of faces of the cylindrical surface type in the 3D CAD model. Finally, the largest possible number of candidates can be obtained by summing the above two equations:

$$n_{\mathrm{C}} = n_{\mathrm{POSC}} + n_{\mathrm{AOSC}} = \frac{n_{\mathrm{PL}}\left(n_{\mathrm{PL}} - 1\right)}{2} + n_{\mathrm{CY}} + 6 \,, \tag{1.19}$$

In the above equation the "6" stands for three POSCs and three AOSCs generated from the principal axes of inertia. The number of candidates after the trimming process is difficult to estimate as it depends on how many candidates are eliminated as duplicates and how many of them are above the maximum allowed distance from the COG. An estimation of the final number of POSCs and AOSCs shall be determined later in this study by testing on 3D CAD models. The flowchart of the described procedure is shown in Figure 1.
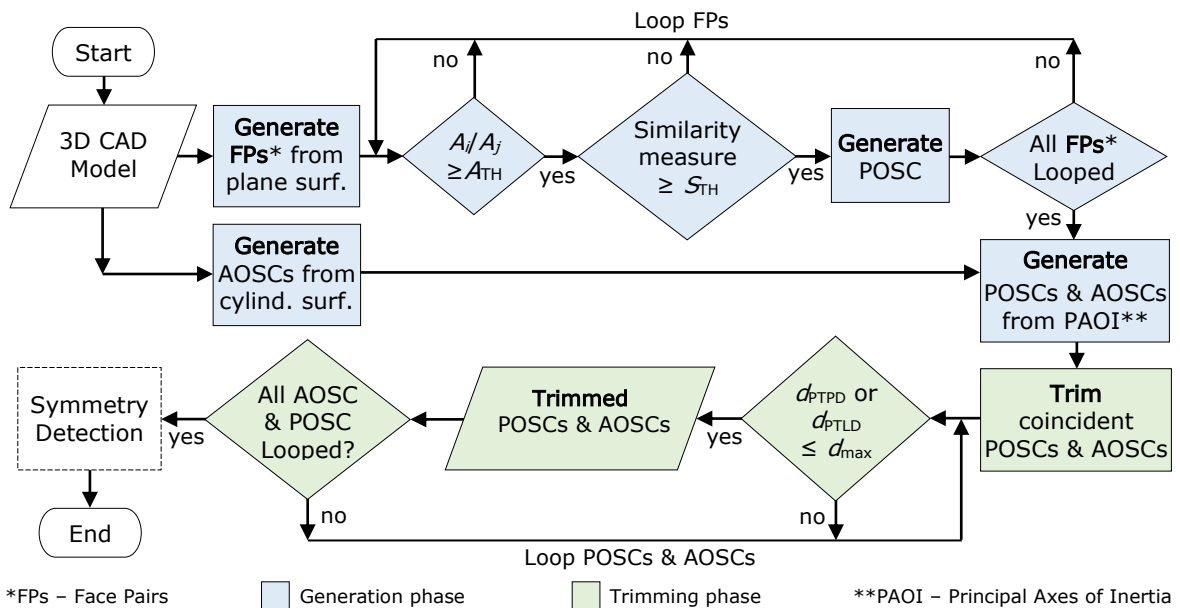
Figure 1: Flowchart of the proposed procedure for identifying the POSCs & AOSCs.

4   VALIDATION OF THE PROPOSED PROCEDURE

First, several similarity measures were compared to select the most suitable, and an estimation of the maximum distance for candidate trimming was conducted. Based on that, the proposed procedure for identifying the POSCs and AOSCs was validated in terms of does it correctly detects all those POSCs and AOSCs which represent also the APOS and AAOS. Further, the number of identified candidates was compared with existing CASD techniques for B-rep CAD models. To estimate the maximum candidate trimming distance and validate the proposed procedure a sample of 300 non-symmetric, exact global and partial, reflectional and axisymmetric 3D CAD models has been collected. All 3D CAD models were in STEP file format, containing a single body and manifold geometry. The types of CAD models included in the sample were: machined, sheet metal, injection mold, forged, and cast parts. The sample was split into two halves, 150 CAD models were used for estimating the maximum candidate trimming distance and 150 for the validation of the procedure.

4.1   Selection of an Appropriate Similarity Measure

The similarity measures JS, CS, SDC, SSC, and BBC have been investigated to explore their applicability for pairing two similar faces. As already stated, the application of similarity measures originates from statistics and is exploited to assess the similarity between finite data sets. Hence, within the context of this study, the faces of the B-rep CAD model are observed as finite sets of

edges. For computing the similarity measure, the faces (of the plane surface type) first need to be decomposed into edges and labeled by a string code (e.g., "oLI10"), as shown in Figure 2.
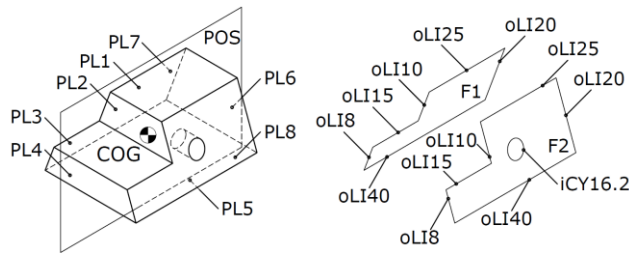

Figure 2: An example of a part and the designation of its faces and edges.

The first letter of the string code indicates whether the edge belongs to an *outer* "o" or *inner* "i" loop. The next two letters describe the edge's underlying curve type, "LI" for line, "CI" for circle, "EL" for ellipse, "BC" for B-spline curve, and so on. Finally, the last part of the designation represents the length of the curve in millimeters. The string code represents a unique label of topological elements, i.e., edges, considering the properties of the underlying geometrical elements (loop type, curve type, and curve length). After designation, in the next step, for each face pair two binary *feature vectors* are created (an example is shown in Table 1), which are used as input for the calculation of the similarity measures. The two feature vectors are of equal dimension corresponding to the number of unique edges across both faces. In each feature vector, the edges are assigned "1" if they are present in the corresponding face and "0" if they are absent. To estimate the applicability of the similarity measures, ten test cases with varied similarities have been selected (Table 2).

Edges	*oLI8*	*oLI10*	*oLI15*	*oLI20*	*oLI25*	*oLI40*	*iCY16.2*
Face 1 – feature vector A	1	1	1	1	1	1	0
Face 2 – feature vector B	1	1	1	1	1	1	1

Table 1: An example of the binary feature vectors for the face pair in Figure 2.

The test cases were selected randomly and based on engineering judgment they can be classified as absolutely similar (Table 2, a), similar (Table 2, c – i), and non-similar (Table 2, j). The computed scores for the similarity measures are given in Table 2. The results show that all similarity measures correctly recognize absolutely similar (Table 2, a) and non-similar face pairs (Table 2, j). The test cases also show why the ratio of surface areas A_i/A_j may not be an effective metric for measuring similarity, because two geometrically different shapes may have the same surface area values (Table 2, j). Based on the test examples, the threshold value A_{TH} can be set to $A_{TH}=0.90$ (with included safety margin).

All mentioned similarity measures from Equations (1.3) to (1.7) have the same numerators comprising the number of common features in both data sets, while the main difference between them derives from the denominators. The JI is the most conservative similarity measure compared to others as the computed scores are always the lowest. By its definition, the JI stronger penalizes differences between two sets of edges, even if one is a proper subset of the other (Table 2, e). This is because the JI considers in the denominator the total membership of both sets of edges. Slightly lower than the JI, the BBC also penalizes differences in the size of the sets as the number of common edges is divided by the larger size between the two sets of edges. The SDC essentially doubles (i.e., "weights") the intersection in the numerator and divides it with the sum of the cardinalities from both sets of edges.
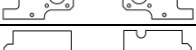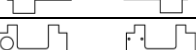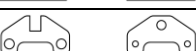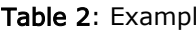
	Face pairs		A_i/A_j	CS	JI	SDC	SSC	BBC
a)			1	1	1	1	1	1
b)			0.96	0.80	0.67	0.80	0.80	0.80
c)			0.98	0.69	0.52	0.67	0.80	0.60
d)			0.97	0.95	0.90	0.95	0.95	0.95
e)			0.98	0.91	0.83	0.91	1	0.83
f)			0.99	0.77	0.61	0.76	0.92	0.65
g)			0.96	0.92	0.84	0.91	0.94	0.89
h)			0.94	0.76	0.61	0.76	0.81	0.71
i)			1	0.75	0.60	0.75	0.75	0.75
j)			1	0	0	0	0	0

Table 2: Example of face pairs and the computed similarity measures.

Consequently, this produces less penalization and higher similarity than in the case of the JI and BBC. The difference between the CS and SDC is negligible because their denominators, $\sqrt{(|X| \cdot |Y|)}$ against $0.5(|X|+|Y|)$, will result in nearly identical scores, as long as the number of edges in both faces does not differ considerably (i.e., the difference is not bigger than one order of magnitude). The SSC is the least conservative similarity measure, which in certain cases may result in a false positive identical face pair. This happens if all edges in the "smaller" face are also found in the "larger" face (Table 2, e), then SSC is 1 regardless of how many additional edges are in the "larger" face. Based on the computed scores for the given test cases, it can be concluded that the JI and BBC are not adequate to measure the similarity between two faces due to the considerable penalization leading to an underestimation of similarity, while the SSC in some cases may overestimate the similarity. Hence, the CS and SDC, which both produce nearly identical scores, represent the most convenient measure of similarity between two faces. To consider a face pair similar, the condition CS≥S_{TH} or SDC≥S_{TH} needs to be fulfilled, whereby the threshold value can be set to S_{TH}=0.75 (considering the computed examples in Table 2). The CS was used for the validation of the proposed procedure.

4.2 Estimating the Maximum Distance for Candidate Trimming

Candidate trimming is a crucial phase that enables a further reduction of the number of initially generated candidates. Hence, the computed PTPD and PTLD are queried against an empirically defined maximum distance d_{max} to judge if the POSCs or AOSCs should be trimmed or not. If d_{max} is too high, many candidates may remain untrimmed, if it is too low, many candidates could be trimmed among which may also be the APOSs or AAOSs. Therefore, the basic idea is to determine the maximum allowed distance as a function of the 3D CAD model's minimum bounding box (the smallest box in which the 3D CAD model fits):

$$d_{max} = k \cdot D = k \cdot \sqrt{(\Delta L_x)^2 + (\Delta L_y)^2 + (\Delta L_z)^2} ,$$ (1.20)

where ΔL_x, ΔL_y, and ΔL_z represent the lengths of the 3D CAD model's bounding box in the respective x, y, and z directions, and k is the unknown constant to be determined. The constant k was determined empirically from the first sample of 3D CAD models. For each 3D CAD model, the

$k=d/D$ value is plotted in a graph (Figure 3), where d is the distance of the POSC or AOSC from the COG, and D is the diagonal of the bounding box.
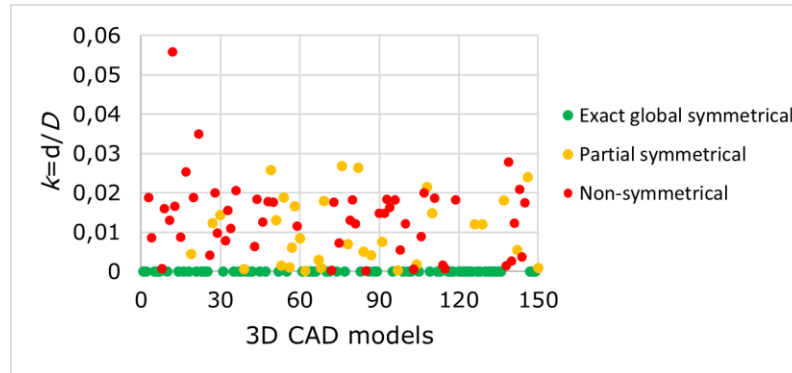

Figure 3: Plot of the parameter k for each 3D CAD model.

The 3D CAD models were divided into three groups: exact global, partial, and non-symmetrical (asymmetrical). Obviously, for exact global symmetrical 3D CAD models, the distance of the POSC or AOSC from the COG will always be $d=0$, which means that $k=0$. For partial symmetrical and non-symmetrical 3D CAD models $k>0$, where the results show that all partial symmetrical objects fall into $k<0.03$. Hence, to be on the safe margin, the parameter k can be set to $k=0.05$. In other words, in the case of partial symmetry, the 3D CAD model's APOS or AAOS will be maximumly distanced from the COG within 5% of its bounding box diagonal length. Finally, the equation (1.17) for computing the maximum allowed distance of the POSC or AOSC from the COG turns into:

$$d_{max} = 0.05 \cdot \sqrt{\left(\Delta L_x\right)^2 + \left(\Delta L_y\right)^2 + \left(\Delta L_z\right)^2} \ . \tag{1.11}$$

4.3 Testing of the Proposed Procedure

The proposed procedure for identifying the POSCs and AOSCs has been implemented into a CAD system using its Application Programming Interface (API) and tested on the second sample of 150 CAD models. The CAD models subjected to testing were exact global symmetrical (including those exhibiting multiple reflectional symmetries misaligned with the PAOI), partial symmetrical, and non-symmetrical. The scope of testing was to determine the correctness of detecting the respective POSCs and AOSCs, where correct indicates that among the detected candidates there are also the APOS or AAOS (later to be detected by the symmetry detection procedure). Further, the testing has been exploited to estimate the number of generated candidates and compare it with existing symmetry detection techniques for B-rep CAD models.

4.3.1 Implementation of the procedure

The CAD system exploited for the implementation of the procedure was Solidworks 2020 through its API functionalities. At the beginning of the candidate generation phase, all faces of the plane and cylindrical surface type are grouped into classes. All faces in a body can be retrieved by *Body2.GetFaces()* method (*Body2* indicates the interface, *GetFaces* the method, same analogy will be used for the following commands). The area of a face can be retrieved from *Face2.Area()*. The underlying surface of each face is obtained using *Face.GetSurface ()*, while the type of surface is obtained with the *Surface.Identity()* method. To generate the AOSCs, all faces of the cylindrical surface type are looped once. Finally, each AOSC is defined from the cylindrical surface parameters *Surface.CylinderParams()*, i.e., an axis vector and a point on it. The POSCs are generated by pairwise comparison of plane surfaces. First, the normal for each face needs to be retrieved with *Surface.PlaneParams ()*. The centroid of a face can not be directly acquired, but a workaround solution needs to be applied (the same applies to the edge midpoint). A face (or edge) needs to be

selected to insert a reference point with *FeatureManager.InsertReferencePoint()*. This reference point represents the centroid (or edge midpoint). Next, to compute the similarity measure, each face is decomposed into edges. This is accomplished through the face's loops and then via the loop's edges, i.e., *Face2.GetLoops ()* → *Loops.GetEdges(). Loop.IsOuter()* reveals the loop type (outer or inner). The underlying curve of an edge is retrieved with *Edge.GetCurve()*, while the type of curve with *Curve.Identity()*. The length of the edge is computed from the underlying curve using *Curve.GetLength2()* method. The mentioned methods are used to compute the feature vectors and the similarity measure (Cosine similarity or Sørensen–Dice). If the computed similarity measure is above the threshold value, the face pair is further used to generate the POSC, using Equations (1.8) to (1.14), else it is rejected. For the second phase, candidate trimming, the COG is computed from *ModelDocExt.GetMassProperties2()*. Based on that, the PTPD or PTLD are computed for each POSC or AOSC.

4.3.2 Results

Test results show that the procedure identifies in approx. 95% of test cases the correct POSCs and AOSCs, among which are also the APOS and AAOS. In only 5% of test cases, when the reflectional symmetric CAD models do not have any faces of the plane surface type (Figure 4), the procedure fails to detect the respective POSCs (the typical CAD models where this happens are for instance gears, flanges, etc.). Consequently, the symmetry detection procedure would later fail to detect the APOS.
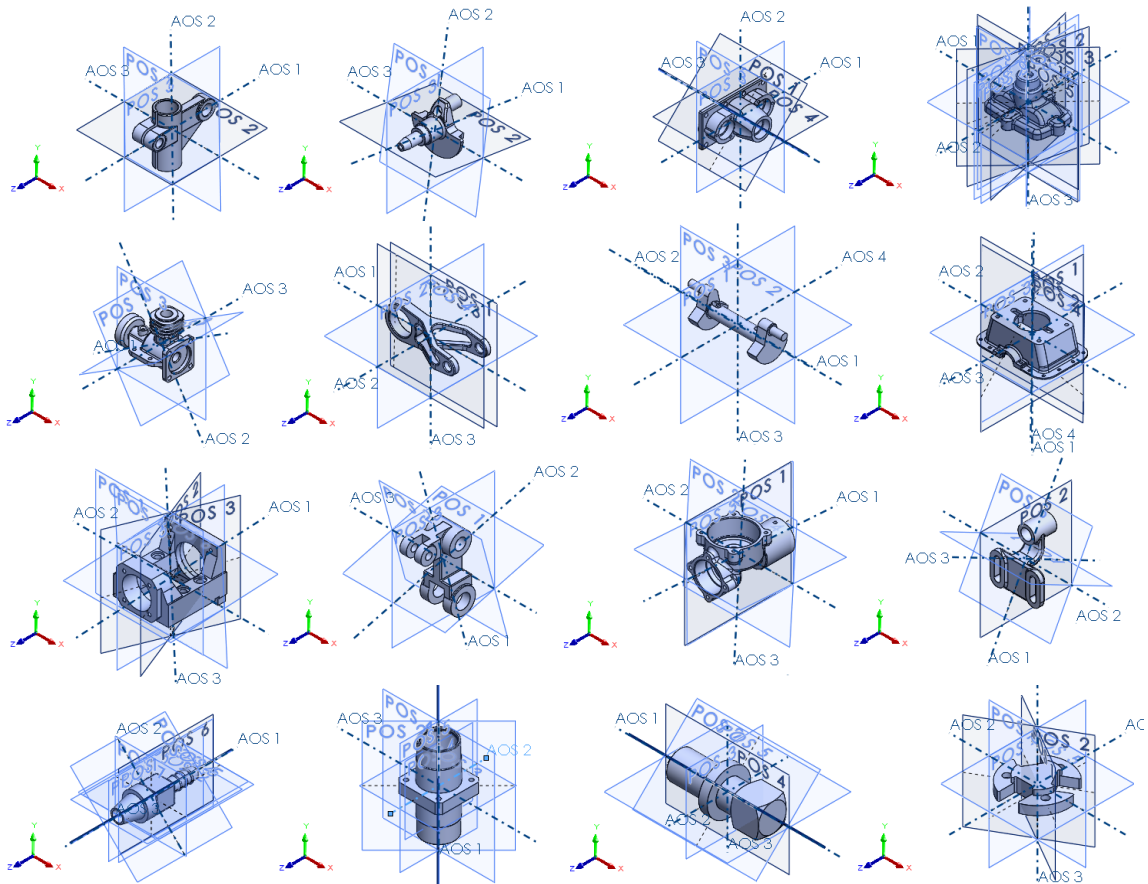

Figure 4: Examples of the CAD models subjected to testing and the obtained POSCs and AOSCs.
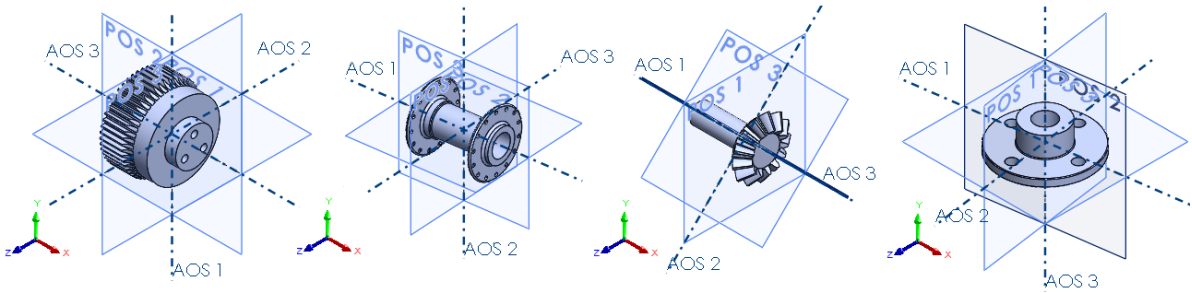
Figure 5: Examples of 3D CAD models where the corresponding POSCs have not been detected completely.

When it comes to the number of POSCs and AOSCs, the proposed procedure results in an average number of 1141 initially generated candidates, while after trimming, the average number of POSCs and AOSCs per 3D CAD model is only 15. That means the trimming phase reduces the number of candidates (approx. 76 times). Also, Table 3 compares the generated number of candidates with existing studies, again in terms of the average number of candidates per CAD model. Compared to *Li et al.* [11][12], the present study produces ≈105 times fewer POSCs and AOSCs and respectively ≈138 times less than *Tate et al.* [26][27].

CASD technique	Equation	Average initial n_c per CAD model	Average n_c per CAD model used as input for the symmetry detection
Li et al. [11][12]	(1.1)	1572	1572*
Tate et al. [26][27]	(1.2)	20766	2077**
This study	(1.19)	1141	15***

* The initially generated candidates are also used as input for symmetry detection.
** After the rationalization of candidates. Estimated 10% of the initially generated candidates, the exact number is difficult to estimate.
*** After trimming of candidates.

Table 3: Comparing the average number of candidates n_c between different CASD techniques.

5 CONCLUSIONS

This paper addresses the identification of the planes and axes of symmetry candidates in B-rep CAD models. The procedure consists of two phases: *generating* and *trimming* candidates. The AOSCs were *generated* from single faces with the underlying cylindrical surface type, while the POSCs were generated from similar face pairs (plane surface type), which were identified using a similarity measure. For selecting the most convenient similarity measure, five of them were investigated. Based on that, it can be concluded that the Cosine similarity or Sørensen–Dice coefficient represents the most promising choices, both providing nearly identical scores. The *trimming* of candidates implies eliminating duplicates and those that are considerably distanced from the COG. The procedure has been tested on a sample of 300 CAD models and the results show that it identified the correct candidates (representing also the actual planes and axes of symmetry) in 95% of test cases. The average number of candidates per 3D CAD model is only 15. Compared to other CASD techniques, the proposed procedure significantly reduces the number of candidates, which is an important factor for reducing computational complexity. The present study applies to simpler CAD models with numeric surfaces that might be generated unintentionally as a result of rounding and chamfering of edges. Such numeric surfaces do not contribute dominantly to the overall symmetry in the CAD model and were therefore not used for the generation of POSCs.

The procedure is not intended to detect candidates in CAD models that are mainly or entirely compound of complex numeric surfaces. Future research will be focused on addressing the main disadvantage of the procedure, i.e., its extension for identifying the POSCs in case the 3D CAD model does not have any faces of the plane surface type.

Mladen Buric, http://orcid.org/0000-0001-8921-6024
Stanko Skec, https://orcid.org/0000-0001-7549-8972

REFERENCES

[1] Buric, M.; Brcic, M.; Bojcetic, N.; Skec, S.: Computer-Aided Detection of Exact Reflection and Axisymmetry in B-rep rep CAD Models. Computer-Aided Design and Applications, 20(5), 2023, 884-897, https://doi.org/10.14733/cadaps.2023.884-897

[2] Buric, M.; Brcic, M.; Bojcetic, N.; Skec, S.: Computer-Aided Detection of Exact Reflection and Axisymmetry in B-rep CAD Models. Conference: CAD'22, Beijing, China, 11-13 July 2022. https://doi.org/10.14733/cadconfP.2022.251-256

[3] Cardone, A.; Gupta, S. K.; Deshmukh, A.; Karnik, M.: Machining feature-based similarity assessment algorithms for prismatic machined parts, Computer-Aided Design, 38(9), 2006, 954-972, https://doi.org/10.1016/j.cad.2006.08.001

[4] Chaudhari, A. ; Bilionis, I. ; Panchal, J.: Similarity in Engineering Design: A Knowledge-Based Approach, Proceedings of the ASME 2019 International Design Engineering Technical Conferences and Computers and Information in Engineering Conference. Volume 7: 31st International Conference on Design Theory and Methodology. Anaheim, California, USA. August 18–21, 2019. V007T06A045. ASME. 2019, https://doi.org/10.1115/DETC2019-98272

[5] Chen; Y.; Linzi, F.; Feng, J.: Automatic and Exact Symmetry Recognition of Structures Exhibiting High-Order Symmetries, Journal of Computing in Civil Engineering, 2018, 32(2), https://doi.org/10.1061/(ASCE)CP.1943-5487.0000743

[6] Giesecke, F. E.; Lockhart, S.; Goodman, M.; Johnson, C.: Technical Drawing with Engineering Graphics 15th edition, Pearson Education, US, 2016

[7] Hruda, L.; Kolingerová, I.; Lávička, M.: Plane Space Representation in Context of Mode-Based Symmetry Plane Detection, ICCS 2020: Computational Science, 2020, 509-523, https://doi.org/10.1007/978-3-030-50426-7_38

[8] Hruda, L.: Symmetry Detection in Geometric Models, Master Thesis, University of West Bohemia, Plzen, Czech Republic, 2018

[9] Hruda, L.; Dvorák, J.: Estimating Approximate Plane of Symmetry of 3D Triangle Meshes. Proc. Central European Seminar on Computer Graphics, Smolenice, Slovakia, 2017.

[10] Kakarala, R.; Kaliamoorthi, P.; Premachandran, V.: Three-dimensional bilateral symmetry plane estimation in the phase domain. Proceedings of the IEEE Conference on Computer Vision and Pattern Recognition, 2013, 249–256. https://doi.org/10.1109/CVPR.2013.39

[11] Li, K. ; Foucault, G.; Leon, J.; Trlin, M.: Fast global and partial reflective symmetry analyses using boundary surfaces of mechanical, Computer Aided Design, 53, 2014, 70-89. https://doi.org/10.1016/j.cad.2014.03.005

[12] Li, K.: Shape Analysis of B-Rep CAD Models to Extract Partial and Global Symmetries, PhD Thesis, University Grenoble, 2011

[13] Li, B.; Johan, H.; Ye, Y.; Lu Y.: Efficient 3D reflection symmetry detection: A view-based approach. Graphical Models. 2016, 83, 2–14. https://doi.org/10.1016/j.gmod.2015.09.003

[14] Lipman, Y.; Chen, X.; Daubechies, I.; Funkhouser, T.: Symmetry factored embedding and distance. ACM Transactions on Graphics, 2010, 29(4), 1–12. https://doi.org/10.1145/1778765.1778840

[15] Ma, Z.; Zhang, T.; Liu, F.; Yang, J.: Knowledge discovery in design instances of mechanical structure symmetry, Advances in Mechanical Engineering, 7(11), 2015, 1-19. https://doi.org/10.1177/1687814015615044

[16] Martinet, A; Soler, C.; Holzschuch, N.; Sillion. F.X.: Accurate Detection of Symmetries in 3D Shapes. ACM Transactions on Graphics, 2006, 25 (2), 439 - 464. https://doi.org/10.1145/1138450.1138462

[17] Mitra, N.J., Pauly, M., Wand, M. and Ceylan, D.: Symmetry in 3D Geometry: Extraction and Applications. Computer Graphics Forum, 32, 2013 1-23. https://doi.org/10.1111/cgf.12010

[18] Mitra, N. J.; Guibas, L. J.; Pauly, M. Partial and approximate symmetry detection for 3D geometry. ACM Transactions on Graphics, 2006, 25, 560–568. https://doi.org/10.1145/1179352.1141924

[19] Parry-Barwick, S.; Bowyer, A: Symmetry analysis and geometric modelling. Proceedings DCTA'93, Digital Image Computing-Techniques and Applications, Sydney, Australia, 1993.

[20] Qiu, Q.; Chen, X.; Yang, C.; Feng, P.: Classification and Effects of Symmetry of Mechanical Structure and Its Application in Design, Symmetry, 13(4), 2022, 683. https://doi.org/10.3390/sym13040683

[21] Seifoddini, H.; Djassemi, M.: Merits of the production volume based similarity coefficient in machine cell formation, Journal of Manufacturing Systems, 1995, 14(1), 35-44, https://doi.org/10.1016/0278-6125(95)98899-H

[22] Schiebener, D.; Schmidt, A.; Vahrenkamp; N.; Asfour, T.: Heuristic 3D object shape completion based on symmetry and scene context, 2016 IEEE/RSJ International Conference on Intelligent Robots and Systems (IROS), Daejeon, South Korea, 2016, 74-81, https://doi.org/10.1109/IROS.2016.7759037

[23] Sipiran, I.; Gregor, R.; Schreck, T.: Approximate symmetry detection in partial 3D meshes. Computer Graphics Forum, 2014, 33, 131–140. https://doi.org/10.1111/cgf.12481

[24] Stephenson, M.; Clark, A.; Green, R.: Novel methods for reflective symmetry detection in scanned 3D models. 2015 IEEE International Conference on Image and Vision Computing, New Zealand, 2015, 1–6. https://doi.org/10.1109/IVCNZ.2015.7761555

[25] Sun, C.; Sherrah, J.: 3D symmetry detection using the extended Gaussian image, IEEE Transactions on Pattern Analysis and Machine Intelligence. 1997, 19(2), 164–168. https://doi.org/10.1109/34.574800

[26] Tate, S.; Jared, G.: Recognising symmetry in solid models, Computer-Aided Design, 35, 2003, 673-692. https://doi.org/10.1016/S0010-4485(02)00093-3

[27] Tate, S.J.: Symmetry and Shape Analysis for Assembly-Oriented CAD, PhD Thesis, Cranfield University, 2000

[28] Tierney, C.; Boussuge, F.; Robinson, T. ; Nolan, D.; Armstrong, C.: Efficient symmetry-based decomposition for meshing quasi-axisymmetric assemblies, Computer-Aided Design and Applications, 16(3), 2019, 478-495. https://doi.org/10.14733/cadaps.2019.478-495

[29] Wang, J.; Yan, W.; Huang, C.: Surface shape-based clustering for B-rep models, Multimedia Tools and Applications, 7, 2020, 25747–25761, https://doi.org/10.1007/s11042-020-09252-3

[30] Zehtaban, L.; Elazhary, O.; Roller, R.: A framework for similarity recognition of CAD models, Journal of Computational Design and Engineering, 3(3), 2016, 274-285, https://doi.org/10.1016/j.jcde.2016.04.002

[31] Zingoni, A.: Symmetry recognition in group-theoretic computational schemes for complex structural systems, Computers & Structures 2012, 34-44, 94-95. https://doi.org/10.1016/j.compstruc.2011.12.004